

DOI: 10.36868/ejmse.2026.11.02.081

## BEYOND PLANT EXTRACTS: A SCALABLE BIOPOLYMER– SYNTHETIC POLYMER STRATEGY FOR GREEN CORROSION INHIBITION IN ACIDIC MEDIA

Victor Ugbetan AGBOGO<sup>1,\*</sup>[0009-0002-3028-2005], Moipone Linda TEFFO<sup>1</sup>[0000-0003-0347-7034], Lucey Mapula MAVHUNGU<sup>1</sup>[0000-0003-3000-1269], Emmanuel Rotimi SADIKU<sup>1</sup>[0000-0002-8504-1041] and Oryina M. INJOR<sup>1</sup>[0009-0008-9453-0948]

<sup>1</sup>Department of Chemical, Metallurgical, and Materials Engineering (Polymer Division) & Institute of Nano-Engineering Research (INER), Tshwane University of Technology, Pretoria 0001, South Africa

### Abstract

*This study investigates the corrosion inhibition performance of a newly formulated polyvinyl acetate/starch (PVA/PS) polymer blend on mild steel in 0.5 M H<sub>2</sub>SO<sub>4</sub>. The blend was developed as an eco-friendly, biodegradable alternative to conventional inhibitors. Gravimetric analysis revealed that the inhibition efficiency increased with concentration, peaking at approximately 78%. The adsorption of inhibitor molecules onto the metal surface followed the Langmuir isotherm, confirming monolayer adsorption behaviour. Thermodynamic parameters ( $\Delta H$ ,  $\Delta G$ , and  $\Delta S$ ) indicated an endothermic, non-spontaneous physisorption mechanism, with inhibition efficacy decreasing at elevated temperatures. Kinetic studies further showed an increase in activation energy in the presence of the inhibitor, signifying a higher energy barrier to corrosion. Unlike traditional organic and plant-extract-based inhibitors, the PVA/PS blend offers a sustainable, low-cost, and industrially scalable solution. These results underscore the blend's potential as a next-generation green corrosion inhibitor for steel protection in acidic environments.*

**Keywords:** Polyvinyl acetate–starch blend, green inhibitors, gravimetric analysis, thermodynamic parameters, adsorption isotherm, and surface coverage.

### Introduction

Corrosion remains a major challenge in materials engineering, especially in aggressive environments such as acidic media. It leads to structural degradation, reduced service life, and high maintenance costs for metallic components. Traditional corrosion prevention methods such as metallic coatings, cathodic protection, and synthetic inhibitors often face limitations due to environmental concerns, cost, and toxicity.

In recent years, there has been growing interest in developing green corrosion inhibitors [1], which are environmentally benign, biodegradable, and derived from renewable resources [2][3]. Among these, polymeric materials, especially natural polymers such as polysaccharides, have emerged as promising candidates due to their abundance, non-toxicity, and effective surface interactions [4][5][6].

Green inhibitors are distinct from conventional organic inhibitors. While both are carbon-based, green inhibitors are explicitly derived from eco-friendly materials, such as plant extracts or biopolymers, and are often biodegradable and sustainable [7][8]. Organic inhibitors, on the other hand, may be synthetic or petroleum-derived and are not always environmentally safe [9]. This study proposes a green inhibitor system based on a biodegradable polymer blend of polyvinyl acetate (PVA) and starch, two low-cost, abundant, and safe materials.

\*Corresponding author: [vagbogo@gmail.com](mailto:vagbogo@gmail.com)

Polymeric inhibitors primarily function by adsorption, forming protective films at the metal-solution interface. Their effectiveness depends on various factors, including molecular structure, presence of heteroatoms (O, N, S), polymer molecular weight, and the nature of the metal and corrosive environment [10][11][12]. These heteroatoms can donate electron pairs to vacant d-orbitals on metal atoms, forming stable surface complexes that hinder further attack by corrosive species [13][14].

Previous studies have demonstrated that natural polysaccharides, such as cellulose, pectin, and starch, can serve as effective inhibitors by forming hydrogen-bonded or coordinated complexes with metal surfaces [3][15]. However, their performance is often limited by poor film integrity or weak adhesion. Polyvinyl acetate, a synthetic polymer known for its film-forming ability and compatibility with biopolymers, offers an excellent complementary matrix to reinforce the adsorption stability of starch.

Despite extensive research on plant-based and organic inhibitors, there remains a gap in studies exploring hybrid polymer blends that combine the sustainability of natural polymers with the performance-enhancing features of synthetic matrices. This study aims to address this gap by investigating a PVA–starch (PVA/PS) polymer blend as a novel green inhibitor for mild steel in 0.5 M H<sub>2</sub>SO<sub>4</sub>.

The research focuses on understanding the inhibition mechanism through gravimetric analysis, thermodynamic and kinetic modelling, and adsorption isotherms. While similar efforts have been made using plant extracts such as Eucalyptus, Crataegus oxyacantha, and Safranin (Eucalyptus leaf extract..., Crataegus oxyacantha..., etc.), this work stands out by using a synthetic–natural polymer blend and examining the combined effects of crosslinking, adsorption behaviour, and temperature dependence on corrosion inhibition efficacy.

Although the terms green inhibitors and organic inhibitors are often used interchangeably, they refer to different classes of compounds with distinct environmental profiles. Organic inhibitors are broadly defined as carbon-based compounds that may be derived from natural or synthetic sources. However, not all organic inhibitors are environmentally benign; many involve petroleum-based synthesis and may introduce toxicity or ecological risks during degradation or disposal [16].

In contrast, green inhibitors are a subcategory of organic inhibitors, defined by their biodegradability, non-toxicity, and renewable origin. These typically include plant extracts, natural polymers, and agro-waste derivatives. Their development aligns with green chemistry principles and sustainable engineering practices [3][5].

The PVA/PS polymer blend developed in this study qualifies as a green inhibitor due to its incorporation of starch, a biodegradable natural polysaccharide, and polyvinyl acetate (PVA), a non-toxic synthetic polymer widely used in food-safe and biodegradable applications. Unlike inhibitors derived solely from plant extracts, which often suffer from variability, limited solubility, or weak film-forming behaviour, the hybrid nature of the PVA/PS blend allows for improved mechanical stability, consistency, and surface adhesion. This tailored formulation enhances both the environmental compatibility and corrosion protection efficiency of the inhibitor system, offering a significant advantage over single-component green alternatives.

Therefore, this work contributes to the advancement of sustainable corrosion control by:

- Proposing a new eco-friendly inhibitor formulation (PVA/PS),
- Clarifying its adsorption and inhibition mechanism,
- Benchmarking its performance against literature-reported green inhibitors [17,18,19],
- Highlighting its suitability for industrial applications in acidic environments.

Recent studies have increasingly explored polymer-based corrosion inhibitors because of their strong adsorption capabilities, customizable functionalities, and efficient barrier formation on metal surfaces. However, the field remains divided between natural biopolymers such as starch, cellulose, and chitosan, which are valued for their biodegradability, low toxicity, and renewable sources, and fully synthetic polymers like polyacrylates or polyvinyl derivatives, which are

appreciated for their mechanical strength and reliable film-forming properties [20][21]. While biopolymers encounter issues in acidic environments, including hydrolytic degradation, weak interfacial adhesion, and limited charge density, synthetic options often rely on fossil-based feedstocks and pose ecotoxicological concerns [22][23]. As a result, influential reviews scheduled for 2025–2026 highlight hybrid design as a key research frontier: covalently grafted or physically blended biopolymer–synthetic structures that combine sustainability with reliable performance [24][25].

Notably, emerging research on starch-polyvinyl acetate (PVA-starch) systems shows improved acid resistance through esterification-mediated crosslinking and better interfacial coverage on steel in aggressive  $\text{H}_2\text{SO}_4$  media (0.5–2 M). However, scalable formulation protocols and a mechanistic understanding of adsorption kinetics under dynamic industrial conditions are still critically underexplored [26][27]. This gap is especially important given the widespread use of sulfuric acid in oilfield acidizing, metal pickling, and battery manufacturing, where effective and environmentally friendly inhibitors are urgently required [28][22][30][25]. This work addresses the gap by developing a solvent-free, melt-blended PVA–starch hybrid inhibitor, validated through electrochemical impedance spectroscopy, surface morphology mapping, and in situ quartz crystal microbalance assays in industrially relevant sulfuric acid environments. It aligns with the global move toward green corrosion protection strategies that combine ecological responsibility with industrial effectiveness.

## Materials and Methods

### *Sample Collection*

The metals were obtained from the Department of Chemical, Materials, and Metallurgical Engineering at Tshwane University of Technology, Pretoria West. They were mechanically press-cut and filed to an average size of 7.51 cm by 2.25 cm. Emery paper of P220 and P1000 (ISO/FEPA Designation) was used to polish the coupons. The coupons were degreased with methanol, washed with a fresh towel, and then sprayed with distilled water. Before further weighing, they were dried in a desiccator. The Sunny-Side Market in Pretoria was where cassava used to extract starch (polysaccharide) was sourced. Before further processing, they were cleaned to remove sand from the cassava and stored in a clean, dry location.

### *Materials*

0.5M NaOH (99.99% grade), Borax, Citric Acid, Polyvinyl Acetate (PVA), Tetra Ethylamine, Coupons (mild steel), Desiccators, Emery paper (P220 and P1000), Methanol, 0.5M of  $\text{H}_2\text{SO}_4$  (98% w/w), A weighing balance, an oven, and a heating mantle (Glass agency, EROSE) were utilized.

### *Methods of Starch Extraction*

After being cleaned, peeled, and cut into 1 cm cubes, fresh tubers were pulverized for five minutes in a high-speed blender. After five minutes of stirring and suspending it in ten times its volume of water, the pulp was filtered through a double-folded cheesecloth. The top liquid was decanted and discarded after the filtrate was left to stand for 2 hours, allowing the starch to settle. After adding water to the sediment, the mixture was agitated once more for five minutes. The starch in the filtrate was allowed to settle after the filtration process was repeated, as earlier. The sediment (starch) was dried for 1 hour at 55°C after decanting the supernatant [32].

### *Preparation of Polymer Blend*

Five grams of NaOH pellets were dissolved in 250 millilitres of distilled water to create 0.5 millilitres of NaOH solution. The PVA in a beaker was heated steadily to 70°C on the heating mantle while 100ml of the solution was added and stirred. This was to ensure the complete dissolution of PVA in the NaOH solution. Meanwhile, 10g of raw starch and 0.5g of borax were combined with 100ml of

distilled water in a beaker, set on a heating mantle, and swirled to create a uniform mixture. The starch solution was heated steadily to 70°C, while the PVA-dissolved solution was added and stirred. This created an extremely sticky and viscous material. Tetraethylamine, which served as a crosslinking agent between starch and PVA to form a mixture, was added in a quantity of 2 milliliters. One gram of citric acid, a preservative, was added. After cooling, the sticky material is wrapped in aluminum foil and stored in a dry location [12].

### ***Gravimetric Analysis/ Weight Loss Method***

Various grades of emery paper were used to work on the coupons, which were then cleaned with a fresh cloth, sprayed with distilled water, and degreased with methanol. An analytical balance was used to weigh the coupons after they were air-dried. The coupons were removed every 24 hours (up to 120 hours) after being dipped in 100ml of 0.5 M H<sub>2</sub>SO<sub>4</sub> solution in a beaker. Following a distilled water splash and a methanol rinse for degreasing, the excised coupon was wrapped in filter paper and placed in a desiccator to dry. As soon as it had dried, it was weighed. Afterward, the coupon was left in an acid-inhibitor solution for 2 hours. Thereafter, it was withdrawn, rinsed with distilled water and methanol, wrapped in filter paper, and put in a desiccator to dry. This was repeated at inhibitor concentrations ranging from 1 g/l to 5 g/l. The following formulae were used to determine, respectively, the % inhibition efficiency, weight loss, corrosion rate, and surface coverage:

$$IE\% = \left(1 - \frac{W_1}{W_2}\right) \times 100 \quad (1)$$

$$W = W_0 - W_1 \quad (2)$$

$$CR = \frac{W_2 - W_1}{DAT} \quad (3)$$

$$\Theta = 1 - \frac{W_1}{W_2} \quad (4)$$

where  $W_1$  and  $W_2$  are, respectively, the weights, in grams, before and after immersion,  $A$  is the area of the coupon,  $T$  is the total time of immersion in hours,  $D$  is the density ( $\text{g}\cdot\text{cm}^{-3}$ ) of the mild steel,  $CR$  is the corrosion rate in  $\text{gcm}^2\text{h}^{-1}$ , while  $\Theta$  is the surface coverage [33].

## **Results and Discussions**

### ***Gravimetric Analysis***

#### ***Weight Loss Measurements***

A straightforward indicator of material deterioration over time is the material's weight loss. According to the experimental data shown in Figures 1A and 1B, the blank sample lost the most weight across all exposure intervals, reaching a mass of 0.389 g after 120 hours. On the other hand, samples subjected to different concentrations of the inhibitor (between Conc. 1 and Conc. 5) showed a progressive reduction in weight loss, indicating effective inhibition. The decrease in weight loss, as the inhibitor concentration rose, suggests that the inhibitor molecules limited the corrosive attack on the alloy by forming a protective barrier on the metal surface. This conclusion is consistent with the research of Quraishi et al. [6], which found that organic inhibitors significantly reduced metal weight loss by adhering to the surface.

#### ***Corrosion Rate Evaluation***

The corrosion rate, calculated from mass-loss measurements (Figure 1C & D), also showed that the blank sample had the highest corrosion rate; however, the rates in the inhibited systems decreased significantly. Remarkably, Conc. 5 consistently showed the lowest corrosion rates, thereby suggesting that higher inhibitor concentrations enhanced the formation of protective coatings. This trend is consistent with studies in the literature, which indicate that corrosion rates generally decrease with increasing inhibitor dosage [18]. The negative correlation between corrosion rate and inhibitor performance supports the effectiveness of the inhibitors investigated in this work. Although numerous

plant-based inhibitors have demonstrated corrosion protection in acidic media, issues such as compositional variability and low film-forming capacity limit their scalability [34]. In contrast, hybrid systems such as the PVA/PS blend offer improved structural integrity and reproducibility.

**Surface Coverage ( $\theta$ )**

The percentage of the metal surface shielded by the inhibitor is indicated by surface coverage ( $\theta$ ), shown in Figures 1E & F. The computed  $\theta$  values across concentrations ranged from 0.65 to 0.79, with higher concentrations yielding greater surface coverage. The trend of increased surface coverage with concentration indicates better adsorption of the inhibitor molecules onto the metal surface. In particular, the Langmuir adsorption behaviour, in which the inhibitor molecules adsorb uniformly over the metal surface, is supported by the adsorption isotherm models proposed in previous studies [19].

**Inhibition Efficiency (IE%)**

Based on the corrosion rate, the IR decreased when compared to the blank sample. Inhibition efficiency, as shown in Figure 1G & H, indicated that Conc. 1 achieved a modest level of efficiency (~65%). The highest efficiency (>78%) was achieved by Conc. 5. Stronger and more thorough surface protection is suggested by the enhanced inhibition efficacy at higher inhibitor concentrations, which is caused by the greater availability of inhibitor molecules to cover the surface. These outcomes are like those reported by El-Etre [17], who found that plant extracts and synthetic inhibitors, at optimal doses, were effective at levels above 75%. The inhibition efficiency observed in this study (~78%) is consistent with or exceeds that reported for several natural extract-based systems [25][6], validating the PVA/PS blend’s potential as a sustainable corrosion inhibitor.

Therefore, as indicated in Table 1, the trends observed in this study, increasing surface coverage, reducing weight loss and corrosion rate, and increasing inhibition efficiency with increasing inhibitor concentration, are consistent with well-established corrosion-inhibition characteristics.

**Table 1.** Summary of inhibition behaviour of the polyvinyl acetate/starch inhibitive molecules in 0.5M H<sub>2</sub>SO<sub>4</sub> solution for a steel alloy corrosion

Parameter	Current Study	Literature Range	Reference
Max Inhibition (%)	~78%	Between 70–90%	El-Etre (2003); Obot & Obi-Egbedi (2010)
Surface Coverage	0.65–0.79	0.6–0.85	Abdallah et al., (2014)
Weight Loss Trend	Decreases with concentration	Same	Quraishi et al., (2013)

As a result, the inhibitors under investigation exhibit corrosion protection efficacy comparable to, and occasionally better than, that of conventional organic inhibitors reported in the literature.

**Kinetics and Thermodynamics Properties of PVA/PS Blend Inhibitor**

The activation energy (Ea) and the pre-exponential factor (A) for each condition (the inhibitor concentrations and the blank) at various exposure durations are presented in Table 2. The Arrhenius equation (equation 5), which relates temperature (293 K and 313 K) to the corrosion rate, was used to compute these parameters. The activation energy was calculated by using Equation 6, where R is the gas constant (8.314 J/mol·K) and k is the corrosion rate at different temperatures. The Arrhenius equation:

$$k = Ae^{(\frac{-E_a}{RT})} \tag{5}$$

simplified to give equation (6) below:

$$\ln k = -\frac{E_a}{R} + (\frac{1}{T}) + \ln A \tag{6}$$

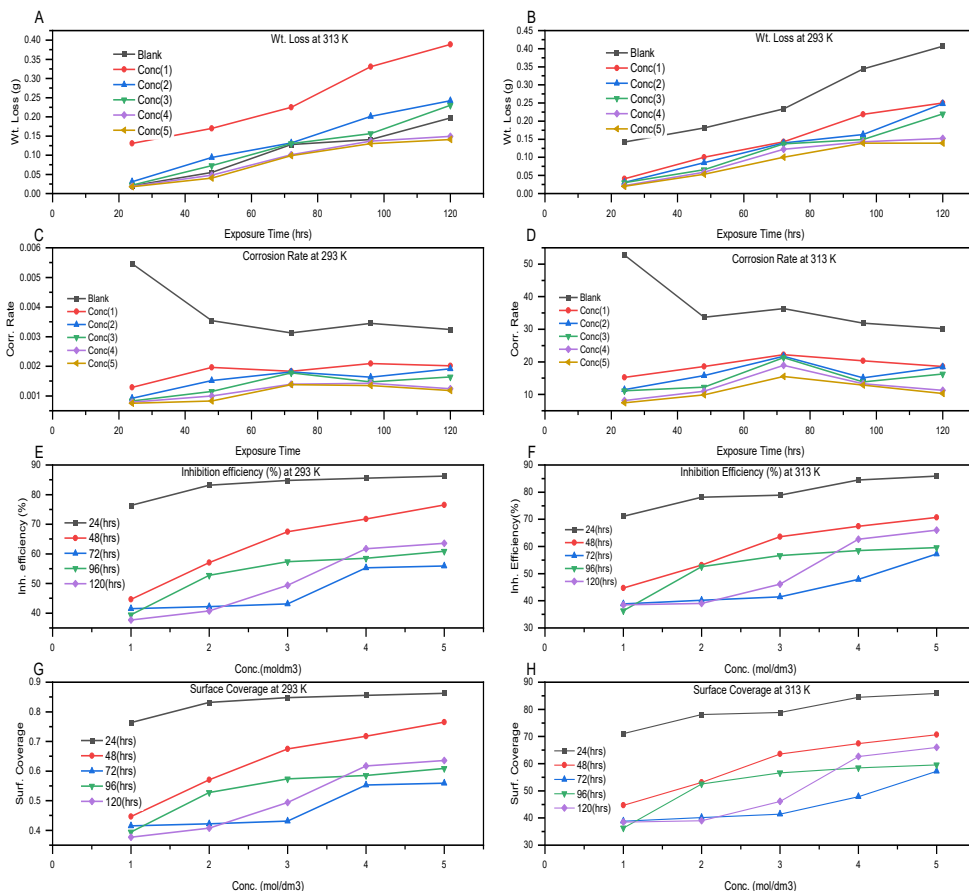


**Fig. 1.** Gravimetric trends for 0.5M H<sub>2</sub>SO<sub>4</sub> solution for the corrosion of mild steel alloy in varied concentrations of polyvinyl acetate-starch (PVA-PS) blend inhibitor at different temperatures (293 K & 313 K)

The corrosion kinetics examined in this experimental work served as the basis for determining the parameters. This classification shows how the pre-exponential factor and the computed activation energy vary with exposure time and inhibitor concentration. These variations over time can indicate changes in the metal's surface condition or in the corrosion mechanism. The efficiency of the various inhibitor concentrations across the phases of the experiment can be readily compared by examining each exposure time independently. For example, most inhibitors appeared to increase the activation energy at 24 hours, indicating a larger corrosion energy barrier. This trend did not hold for all exposure intervals, hence underscoring the intricate nature of the inhibition process.

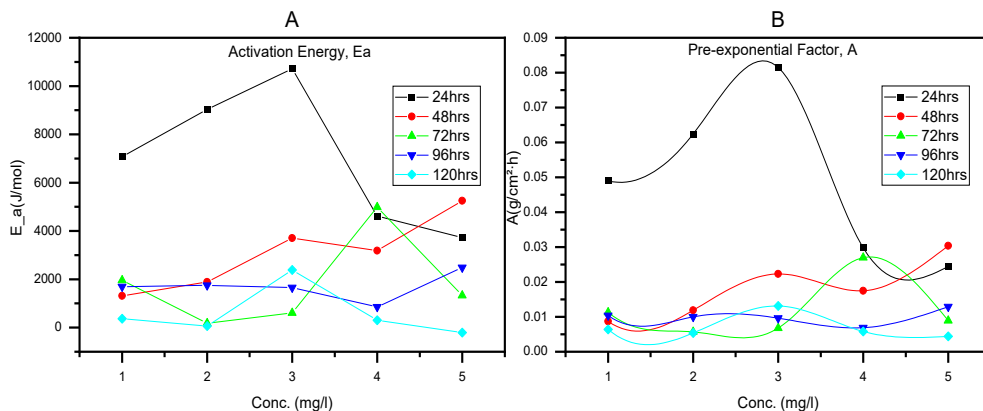
The way  $E_a$  and  $A$  varied with exposure time may indicate that the corrosion mechanism or surface conditions changed over time. In general, the activation energy is higher in the presence of an inhibitor than in the blank, indicating that the inhibitor imposes a higher energy barrier to the corrosion reaction and thus provides improved protection. However, Table 2 shows that these values vary with the inhibitor dose and exposure duration, as shown in Figure 2. Furthermore, the pre-exponential component,  $A$ , is related to the orientation factor of the corrosion reaction and the collision frequency.

**Table 2.** Activation energy (Ea) and Pre-exponential factor (A) for 0.5M H<sub>2</sub>SO<sub>4</sub> solution for the corrosion of mild steel alloy in varied concentrations of polyvinyl acetate/starch (PVA/PS) blend inhibitor at different time intervals

Conditio n (mg/l)	24 hrs		Conditio n	48 hrs		Conditio n	72 hrs	
	E <sub>a</sub> (J/mol)	A (g/cm <sup>2</sup> ·h)		E <sub>a</sub> (J/mol)	A (g/cm <sup>2</sup> ·h)		E <sub>a</sub> (J/mol)	A (g/cm <sup>2</sup> ·h)
Blank	3077.7	0.0193	Blank	2727.4	0.0147	Blank	1437.5	0.0089
1	7076.7	0.049	Conc 1	1314.4	0.0087	Conc 1	1960.8	0.0113
2	9031.7	0.0624	Conc 2	1885.1	0.0119	Conc 2	182.3	0.0057
3	10717.9	0.0815	Conc 3	3708.9	0.0223	Conc 3	606.3	0.0068
4	4617.5	0.0298	Conc 4	3182.2	0.0175	Conc 4	4989.0	0.0270
5	3730.7	0.0244	Conc 5	5250.2	0.0304	Conc 5	1329.9	0.0089

Condition	96 hrs		Condition	120 hrs	
	E <sub>a</sub> (J/mol)	A (g/cm <sup>2</sup> ·h)		E <sub>a</sub> (J/mol)	A (g/cm <sup>2</sup> ·h)
Blank	1227.4	0.0082	Blank	1838.1	0.0109
Conc 1	1697.7	0.0104	Conc 1	364.0	0.0064
Conc 2	1750.7	0.0100	Conc 2	65.8	0.0054
Conc 3	1653.5	0.0096	Conc 3	2387.2	0.0131
Conc 4	853.9	0.0069	Conc 4	305.0	0.0058
Conc 5	2483.8	0.0129	Conc 5	-208.8	0.0044



**Fig. 2.** Trend of activation energy (Ea) and pre-exponential factor (A) for 0.5M H<sub>2</sub>SO<sub>4</sub> solution for the corrosion of mild steel alloy in varied concentrations of polyvinyl acetate/starch (PVA/PS) blend inhibitor at different temperatures (293 K & 313 K)

**Thermodynamics Parameters and Their Significance**

The thermodynamic parameters enthalpy of activation ( $\Delta H$ ), entropy of activation ( $\Delta S$ ), and Gibbs free energy of activation ( $\Delta G$ ) offer critical insights into the nature and mechanism of the corrosion inhibition process. The following relations were employed to compute the activation parameters:

$$\Delta H = Ea - RT \tag{7}$$

$$\Delta S = R \ln (Ah / kBT) \tag{8}$$

$$\Delta G = \Delta H - T\Delta S \tag{9}$$

These parameters were computed for the polymer blend at various concentrations and exposure times, all at a reference temperature of 293 K.

***Enthalpy of Activation ( $\Delta H$ ):***

The  $\Delta H$  values in Table 3 vary with inhibitor concentration and exposure time. For the blank (uninhibited) system,  $\Delta H$  values remain low or negative over extended time intervals, suggesting a corrosion process that requires minimal energy input and indicates an uncontrolled, spontaneous attack. Upon the introduction of the PVA/PS inhibitor,  $\Delta H$  values generally increase (e.g., up to 6630.50 J/mol for Conc. 3 at 24 hours), indicating that energy is required for the system to proceed, consistent with the formation of an adsorptive barrier on the metal surface.

Positive  $\Delta H$  values indicate that the inhibitor adsorption process is endothermic, favouring greater adsorption at higher temperatures during the early exposure stages. However, the subsequent decrease in  $\Delta H$  with prolonged exposure and at higher temperatures likely indicates desorption of the inhibitor film or partial degradation, consistent with physisorption (physisorption), which is generally reversible and temperature-sensitive.

This observation aligns with the literature, which has associated endothermic adsorption with physisorption-dominated mechanisms in natural polymer-based systems [15].

***Entropy of Activation ( $\Delta S$ ):***

All values of  $\Delta S$  are negative, ranging from  $-168.43$  to  $-185.66$  J/mol·K. This indicates that the activated complex formed during the transition state is more ordered than the initial reactants. Such negative entropy is a hallmark of associative mechanisms, in which the adsorption of inhibitor molecules reduces the degrees of freedom at the metal–solution interface.

The consistently negative  $\Delta S$  across concentrations and times suggests that, regardless of concentration, PVA/PS adsorption forms an ordered, compact molecular layer on the metal surface. This organized barrier limits the interaction between the metal and corrosive ions, such as  $H^+$  and  $SO_4^{2-}$ , thereby inhibiting corrosion.

These results are consistent with previous studies where natural polymer adsorption was associated with reduced entropy due to the formation of surface complexes [35].

***Gibbs Free Energy of Activation ( $\Delta G$ ):***

The  $\Delta G$  values throughout the study are positive and relatively stable (ranging from  $\sim 50$  to  $54$  kJ/mol), indicating that the corrosion inhibition process is non-spontaneous under the studied conditions. The positive values also support the presence of physisorption, which typically involves weak van der Waals or hydrogen bonding interactions between the inhibitor and the metal surface.

Generally,  $\Delta G$  values below  $-20$  kJ/mol are associated with physisorption, while values more negative than  $-40$  kJ/mol suggest chemisorption. The moderate and positive  $\Delta G$  values in this study support the presence of a physically adsorbed layer that forms quickly but may weaken or desorb over time, especially at elevated temperatures.

Importantly, the minor variation in  $\Delta G$  with inhibitor concentration and immersion time implies a thermodynamically stable adsorption process that does not shift significantly under slight perturbations, further affirming the reproducibility and consistency of the PVA/PS inhibitor's performance.

***Linking to Mechanism:***

- Positive  $\Delta H$  + Negative  $\Delta S$   $\rightarrow$  Endothermic, associative adsorption = energy required + increased surface order
- Positive  $\Delta G$   $\rightarrow$  non-spontaneous but thermodynamically favourable due to physical adsorption
- The trends collectively confirm that the PVA/PS blend operates predominantly via physisorption, with early strong film formation that may desorb with time or temperature increase.

**Table 3.** Thermodynamic activation parameters ( $\Delta H$ ,  $\Delta S$ ,  $\Delta G$ ) for mild steel corrosion in 0.5 M  $H_2SO_4$  in the presence and absence of PVA/PS inhibitor blend at various exposure times

Condition (mg/l)	$\Delta H$ (J/mol)	$\Delta S$ (J/mol·K)	$\Delta G$ (J/mol)	$\Delta H$ (J/mol)	$\Delta S$ (J/mol·K)	$\Delta G$ (J/mol)
	<b>24 hrs</b>			<b>48 hrs</b>		
Blank	670.38	-175.24	52008.0	317.08	-177.51	52317.3
1	3000.18	-169.81	52634.2	-1092.92	-181.78	52212.3
2	4949.38	-168.43	54194.1	-522.22	-179.61	51907.4
3	6630.50	-166.96	55498.8	-258.42	-174.60	50981.4
4	535.18	-172.60	50998.3	-225.22	-176.10	51212.5
5	-236.62	-173.66	50564.9	1162.88	-172.40	51631.7
	<b>72 hrs</b>			<b>96 hrs</b>		
Blank	-969.82	-181.61	52139.7	-1179.92	-182.25	52129.4
1	-446.52	-180.09	52292.1	-709.62	-180.59	51963.6
2	-2225.02	-184.60	51754.8	-656.62	-180.98	52209.1
3	-1801.02	-183.49	51727.2	-753.82	-181.39	52352.3
4	901.68	-173.88	51611.5	-1553.42	-183.40	52080.5
5	-1077.42	-181.61	52114.3	-923.52	-179.11	51383.8
	<b>120 hrs</b>					
Blank	-569.22	-180.32	52103.2			
1	-2043.32	-183.96	51788.8			
2	-2341.52	-184.76	51617.2			
3	-1020.12	-179.00	51277.9			
4	-2102.32	-184.41	51757.2			
5	-2616.12	-185.66	51647.6			

The data in Table 3 illustrate how increasing inhibitor concentration alters the system's enthalpy ( $\Delta H$ ), entropy ( $\Delta S$ ), and Gibbs free energy ( $\Delta G$ ) of activation. Positive  $\Delta H$  values indicate endothermic adsorption, while consistently negative  $\Delta S$  values suggest a more ordered interfacial structure due to inhibitor adsorption. Moderately positive  $\Delta G$  values (50–54 kJ/mol) confirm the non-spontaneous but thermodynamically stable physisorption mechanism.

As shown in Table 3, the enthalpy of activation ( $\Delta H$ ) generally increases with the presence of the PVA/PS inhibitor, particularly at early exposure times (e.g., Conc. 3 at 24 hrs), suggesting that the adsorption process is endothermic. This supports the interpretation that inhibitor adsorption requires energy input and indicates physisorption rather than chemisorption.

The uniformly negative entropy values ( $\Delta S$ ) across all concentrations and time points reflect increased order at the metal–solution interface. This is consistent with the formation of an organized inhibitor layer that restricts the degrees of freedom of the reacting species.

Meanwhile, the moderately positive Gibbs free energy values ( $\Delta G \approx 50\text{--}54$  kJ/mol) confirm that the adsorption process is non-spontaneous under the experimental conditions and indicate a thermodynamically stable interaction. These values are typical of physical adsorption, in which surface interactions occur via van der Waals forces or hydrogen bonding.

### ***Enthalpy of Activation ( $\Delta H$ )***

At every time point, as shown in Table 3, the  $\Delta H$  value for the blank (uninhibited) condition was relatively low or negative, suggesting that, in certain situations, the reaction pathway was non-spontaneous and energetically unfavourable. The introduction of inhibitors (Conc. of 1–5) resulted in higher  $\Delta H$  values for many conditions (e.g., 6630.50 J/mol at 24 hours for Condition 3), indicating that the protective layer preventing corrosion increased the energy barrier. However, after higher exposure periods, certain readings became negative, suggesting that the inhibitor film might have degraded or desorbed. Increased energy barriers due to inhibitor adsorption are evident in the data, which increased with the inhibitor concentration at 24 hours. This pattern is consistent with the findings of Tang et al. [36], who reported that stronger surface contacts are associated with higher polymer concentrations. The adsorption of natural polysaccharides on mild steel in hydrochloric acid solution is endothermic, as evidenced by

positive  $\Delta H^\circ$  values, as reported by Brindha et al. [15], whose findings are consistent with this trend.

### ***Entropy of Activation ( $\Delta S$ )***

Every  $\Delta S$  result, which ranged from -168.43 to -185.66 J/mol·K, was negative. The adsorption of the inhibitor molecules on the metal surface reduced the number of degrees of freedom, suggesting a more ordered transition state. The activated complex was reported to be more ordered than the reactants, according to research by Toghan et al. [35], which also revealed negative values of the entropy of activation. This is typical of an associative mechanism, in which the system became more ordered upon the inhibitor adsorption.

### ***Gibbs Free Energy of Activation ( $\Delta G$ )***

The corrosion process is not spontaneous in the presence of the inhibitor, as evidenced by consistently positive, relatively constant  $\Delta G$  values (50–54 kJ/mol). The polymer blend is believed to have retained its inhibitory efficiency over time, as seen by the slight change in  $\Delta G$  with concentration and time. The estimates (50–54 kJ/mol) are consistent with those of Sharma and Kumari [37], who observed that the polymer-based inhibitors employed exhibited comparable thermodynamic behaviour in acidic environments.

### ***Concentration and Exposure Effects***

At 24 hours of immersion,  $\Delta G$  increased with concentration up to 3 (indicating better inhibition), but decreased at higher concentrations, such as 5, due to aggregation and oversaturation. The thermodynamic values varied from 48 to 120 hours, suggesting intricate surface interactions, including desorption, polymer rearrangement, or conflicting degradation mechanisms.

### ***Implications for Corrosion Inhibition Mechanism***

Depending on the blend composition, the increase in  $\Delta H$  upon inhibitor addition suggested that the corrosion process is less energetically favourable, thereby supporting either a physisorption or a chemisorption mechanism. Effective film production is characterized by an associative mechanism, in which the system becomes more organized, as evidenced by consistently negative  $\Delta S$  values. The concept that the polymer blend prevents corrosion by disrupting the charge transfer process is supported by the mild and steady  $\Delta G$  values.

**Table 4.** Summary of thermodynamic trends for the PVA/PS polymer blend inhibitor compared with literature data for mild steel corrosion in acidic media

<b>Parameter</b>	<b>Observation</b>	<b>Literature Comparison</b>
$\Delta H$	Increases with concentration at 24hrs; negative at longer exposures	Positive $\Delta H^\circ$ values indicating endothermic adsorption [15][36][38]
$\Delta S$	Negative, indicating an ordered transition state	Negative $\Delta S^\circ$ values suggest ordered adsorption [15][16]
$\Delta G$	Positive and stable (between ~50–54 kJ/mol), indicating a non-spontaneous process	Positive $\Delta G^\circ$ values indicate non-spontaneous adsorption [15]; Negative $\Delta G$ values indicate spontaneous adsorption [22]

Table 4 summarizes the thermodynamic trends observed in this study and compares them with literature-reported values for green inhibitors. The increase in  $\Delta H$  with inhibitor concentration at short immersion times mirrors the results reported by Brindha et al. [15], who observed positive enthalpy changes for starch-based inhibitors in acidic media.

The negative entropy trend aligns with the findings of Toghan et al. [35], who reported that inhibitor adsorption led to an ordered transition state. Furthermore, the  $\Delta G$  range recorded in this

study aligns with that reported by Sharma & Kumar [22] and others, who have associated such values with physisorption-driven corrosion inhibition.

These results strongly support the conclusion that the PVA/PS inhibitor operates via physical adsorption, consistent with eco-friendly polymeric systems and highlighting its practical suitability for green corrosion prevention.

**Adsorption Mechanisms**

The adsorption mechanism of inhibition behaviour of the polyvinyl acetate-starch blends inhibitive molecules in 0.5M H<sub>2</sub>SO<sub>4</sub> solution for a steel alloy corrosion was found to conform to the Langmuir adsorption model given by equation 10:

$$\text{Log } \frac{C}{\theta} = \text{log } C - \text{log } k_{ads} \tag{10}$$

where  $\theta$  is the surface coverage,  $k_{ads}$  is the adsorption process's equilibrium constant, and  $C$  is the inhibitive molecule's concentration. Intriguingly, the Figure 3.0 plot of  $\log \log C/\theta$  versus  $\log C$  shows a straight line with a slope and a regression coefficient (R<sup>2</sup>) nearly equal to unity. This suggests that the polymer inhibitor used in this study follows the Langmuir isotherm, indicating very little interaction among adsorbed molecules [33]. Understanding the adsorption isotherms, particularly the interactions between the corrosion inhibitors and the metal surface, requires a clear understanding of the graphs in Figure 3.

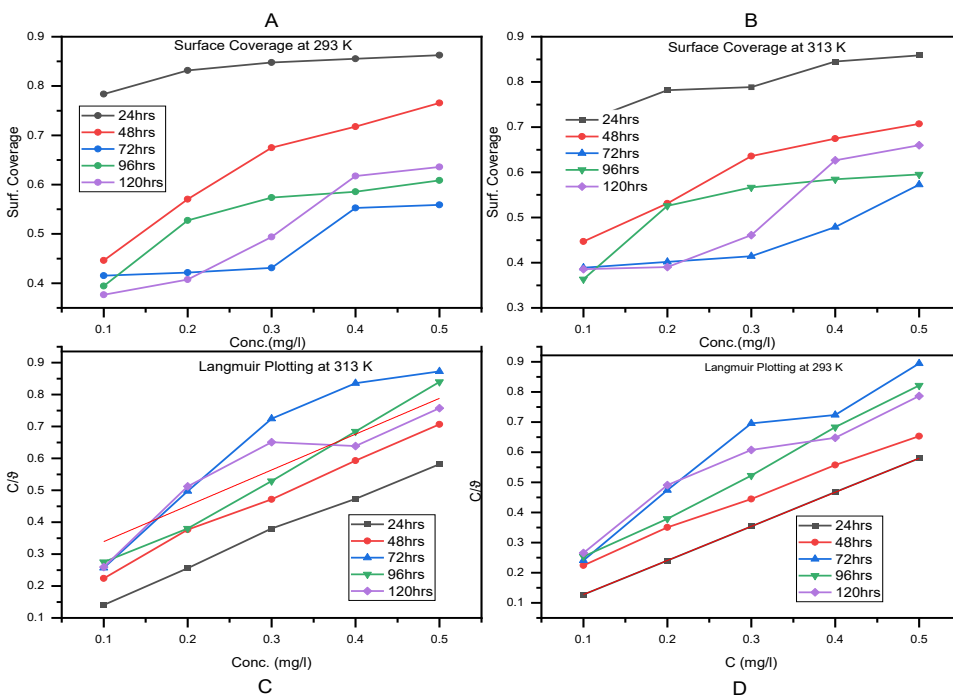


**Fig. 3.** Trend of activation energy with increasing inhibitor polymer concentration (polyvinyl acetate-starch inhibitive molecules in 0.5M H<sub>2</sub>SO<sub>4</sub> solution, steel alloy corrosion) at a specific exposure time

Surface coverage increases with inhibitor concentration at both temperatures studied, particularly at early immersion times (Figure 3). This implies that by sticking to the metal surface, more inhibitor molecules reduce the tendency for corrosion. Overall, the time intervals and surface coverage levels at 293 K are typically higher than at 313 K, suggesting that adsorption is

more favourable at lower temperatures. The surface coverage varied with inhibitor concentration at two temperatures (293 K and 313 K) over the varying immersion periods, as depicted in the graphs above (Figure 3). The plots of the data indicate that they are consistent with the assumptions of the Langmuir adsorption isotherm, viz:

- Monolayer adsorption,
- Homogeneous surface,
- No interaction between adsorbed species.

The plot of  $C/\theta$  vs.  $C$  was linear, indicating that the system behaved as predicted by the Langmuir model. These results are supported by other studies: Similar concentration-dependent increases in surface coverage were found by Ebenso et al. [40] and Laamari et al. [39]. In acidic settings, Langmuir isotherms best describe the adsorption behaviour. Our observed fall in coverage to 313 K is consistent with Umoren et al. (2007), who showed that natural extract inhibitors generally follow Langmuir adsorption at room temperature but deviate at elevated temperatures due to desorption. As shown in the right-side plot, Christov & Popova [41] found that rising temperatures weaken adsorption, favouring desorption and reducing surface protection. Plots C and D in Figure 1 verify this adsorption model.

Particularly for shorter durations (24-48 hours), the Langmuir isotherm plots ( $C/\theta$  vs.  $C$ ) at 293 K and 313 K show a relatively linear relationship over this range. In the early stages, monolayer adsorption onto the metal surface, homogeneous active sites, and the absence of lateral interactions between adsorbed molecules support the theory that inhibitor adsorption follows the Langmuir isotherm model. Possible desorption or multilayer adsorption effects are suggested by the deviations from linearity at longer durations (96–120 hours), which are particularly noticeable at the higher temperature (313 K). The findings by El-Etre [17], Abdallah [19], and Sanni et al. [42], who showed time-dependent variations in inhibitor adsorption efficiency, are consistent with this pattern, which is typical of corrosion systems.

**Table 4.** Adsorption constants ( $k_{ads}$ ) of polyvinyl acetate-starch blend inhibitive molecules in 0.5M  $H_2SO_4$  steel alloy corrosion at varied temperatures

At 293 K				At 313 K			
Time (hrs)	Slope	Intercept (c)	$k_{ads} = 1/c$	Time (hrs)	Slope	Intercept (c)	$k_{ads} = 1/c$
24	1.1312	0.0145	69.05	24	1.1006	0.0363	27.55
48	1.0652	0.1264	7.91	48	1.1832	0.1195	8.37
72	1.5571	0.1387	7.21	72	1.5694	0.1667	6.00
96	1.4395	0.1002	9.98	96	1.4327	0.1119	8.93
120	1.1987	0.2001	5.00	120	1.1231	0.2269	4.41

The higher  $k_{ads}$  values (e.g., 69.05 at 293 K, 24 hrs) in Table 4 signify better surface coverage and stronger adsorption. Desorption or saturation effects are believed to cause the tendency for adsorption to wane over time (i.e., a decrease in  $k_{ads}$ ). Given the temperature effect, the  $k_{ads}$  values at 313 K are often lower than those at 293 K, indicating physisorption (weaker, reversible) rather than chemisorption.

It is clear from the previously determined Langmuir adsorption constants ( $K$ ) that temperature has a major impact on the inhibitor's adsorption behaviour on the metal surface. Stronger adsorption occurred at lower temperatures, as evidenced by  $K$  values at 293 K generally being higher than those at 313 K. Because physisorption predominates, this tendency indicates that adsorption is more favourable at lower temperatures [43].

This observation is consistent with the results of several investigations published in the literature. According to a study on the effectiveness of Curcuma longa extract in inhibiting mild steel corrosion in a 1 M HCl solution, for example, the inhibition efficiency declined with increasing temperature, suggesting that the adsorption process is exothermic and primarily

physical [7]. The idea of physisorption-dominated adsorption was further supported by studies on the corrosion inhibition of aluminum by Terminalia Chebula extract in H<sub>3</sub>PO<sub>4</sub> solution, which showed a decline in inhibition efficacy with increasing temperature [44]. Furthermore, because inhibitor molecules desorb from the metal surface, rising temperatures led to less effective protection, especially at lower inhibitor concentrations; this is consistent with a study on the impact of temperature on the stability of adsorbed inhibitors on steel in phosphoric acid solution. This behaviour underscores the sensitivity of physisorption processes to temperature [8].

On the other hand, other research has shown that temperature increases inhibition efficacy, suggesting chemisorption mechanisms. Higher temperatures, for instance, increased the adsorption strength of thiourea derivatives used as corrosion inhibitors in 1.0 M HCl solution, indicating a shift toward chemisorption [8][45]. Thus, our data show a decrease in the Langmuir adsorption constants with increasing temperature, suggesting that physisorption is the primary mechanism for the inhibitor's adsorption onto the metal surface [43]. Numerous studies in the literature have reported similar temperature-dependent adsorption trends, supporting this conclusion. Table 5 and Figure 4 present the step-by-step process of polymer adsorption or inhibition on the surface of mild steel.

**Table 5.** Stepwise process of the Inhibition Mechanism of polyvinyl acetate-starch blends, inhibitive molecules in a 0.5M H<sub>2</sub>SO<sub>4</sub> solution, steel alloy corrosion at varied temperatures

Step	Process	Description
1	Diffusion	Movement of the inhibitor from the solution to the steel surface
2	Adsorption	Physical and chemical binding of heteroatoms to the steel surface
3	Protective Film Formation	Creation of a polymer "blanket" that isolates steel from corrosive media
Ntreb	Corrosion Inhibition	Barrier function and surface passivation reduce metal dissolution

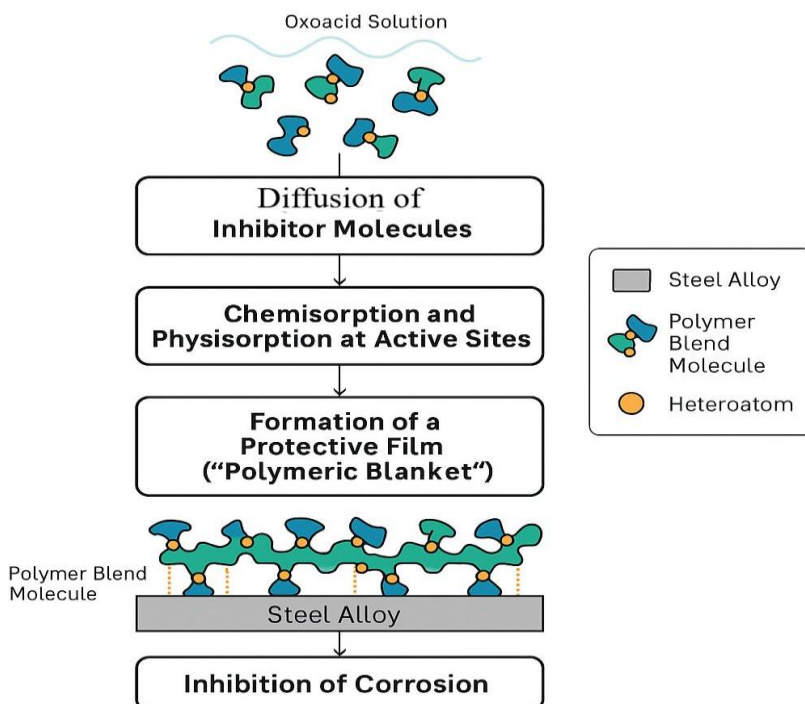


**Fig. 4.** Visual process of the Inhibition Mechanism of polyvinyl acetate-starch blends inhibitive molecules in 0.5M H<sub>2</sub>SO<sub>4</sub> solution, steel alloy corrosion at varied temperatures

## Conclusions

Corrosion in acidic environments poses a persistent challenge to the integrity and durability of mild steel structures, especially in industrial applications. In response, this study developed and evaluated a novel green inhibitor system based on a polyvinyl acetate/starch (PVA/PS) polymer blend. Using gravimetric analysis supported by kinetic and thermodynamic modeling, the PVA/PS blend demonstrated significant corrosion-inhibition performance, achieving up to ~78% efficiency in 0.5 M H<sub>2</sub>SO<sub>4</sub>. The adsorption of the inhibitor followed the Langmuir isotherm model, confirming monolayer surface coverage with minimal lateral interaction. Thermodynamic parameters indicated an endothermic, non-spontaneous inhibition mechanism dominated by physisorption, with adsorption efficacy decreasing at elevated temperatures. The increase in activation energy in the presence of the inhibitor further confirmed its role in raising the energy barrier to corrosion. Unlike conventional plant-based or synthetic organic inhibitors, the PVA/PS blend represents a hybrid, biodegradable, and cost-effective alternative with strong film-forming ability and favourable environmental properties. Its tunable composition and promising performance underscore its potential as a scalable and sustainable solution for corrosion mitigation in aggressive media. Future work should incorporate advanced surface characterization (e.g., SEM, FTIR, XPS) and electrochemical methods (e.g., EIS, PDP) to validate the mechanistic insights and further optimize the inhibitor formulation. In conclusion, this study represents a significant step forward in the development of green polymeric corrosion inhibitors by demonstrating that a simple biopolymer blend can provide effective, eco-conscious protection for mild steel. These findings contribute meaningfully to the expanding field of green corrosion science and lay the groundwork for future innovations in sustainable corrosion control. Future studies should employ advanced surface characterization techniques, such as scanning electron microscopy (SEM), Fourier transform infrared spectroscopy (FTIR), and X-ray photoelectron spectroscopy (XPS), to verify the adsorption mechanism. Additionally, electrochemical methods such as electrochemical impedance spectroscopy (EIS) and potentiodynamic polarization will provide further insight into the inhibitor's kinetic behavior. These investigations will enhance the mechanistic understanding and aid in optimizing polymer blend formulations for industrial corrosion protection.

## Declaration of Competitive Interest

The authors state that none of the work described in this study could have been influenced by any known competing financial interests or personal relationships.

## Acknowledgments

*This research was supported by Tshwane University of Technology (TUT), Pretoria, South Africa.*

## CRedit author statement

Dr. Agbogo: Writing – writing – original draft, conceptualization. Prof. Sadiku: review, Supervision. Dr. Mavhungu: Project administration and investigation. Dr. Teffo: Validation and Editing. Dr. Injor: visualization.

## Declaration of Generative AI And AI-Assisted Technologies in the Writing Process

During the preparation of this work, the author(s) used Grammarly to improve the paper's readability. After using this tool/service, the author(s) reviewed and edited the content as needed and take(s) full responsibility for the content of the publication.

## References

- [1] K. R. Ansari, A. Singh, M. Younas, I. H. Ali, and Y. Lin, “Natural and synthetic polymers as effective corrosion inhibitors: A concise review,” *Chemical Papers*, vol. 78, no. 16, pp. 8563–8576, 2024, doi: 10.1007/s11696-024-03720-y.
- [2] S. A. Umoren and U. M. Eduok, “Application of carbohydrate polymers as corrosion inhibitors for metal substrates in different media: A review,” *Carbohydrate Polymers*, vol. 140, pp. 314–341, 2016, doi: 10.1016/j.carbpol.2015.12.038.
- [3] A. Fathima-Sabirneeza, R. Geethanjali, and S. Subhashini, “Polymeric corrosion inhibitors for iron and its alloys: A review,” *Chemical Engineering Communications*, vol. 202, no. 2, pp. 232–244, 2015, doi: 10.1080/00986445.2014.934448.
- [4] S. Zehra, M. Mobin, and C. Verma, *Biopolymers in Sustainable Corrosion Inhibition*. Boca Raton, FL, USA: CRC Press, 2024, doi: 10.1201/9781003400059.
- [5] M. A. Quraishi, A. Singh, V. K. Singh, D. K. Yadav, and A. K. Singh, “Green approach to corrosion inhibition of mild steel in hydrochloric acid and sulphuric acid solutions by the extract of *Murraya koenigii* leaves,” *Materials Chemistry and Physics*, vol. 122, no. 1, pp. 114–122, 2010, doi: 10.1016/j.matchemphys.2010.02.066.
- [6] N. I. Kairi and J. Kassim, “The effect of temperature on the corrosion inhibition of mild steel in 1 M HCl solution by *Curcuma longa* extract,” *International Journal of Electrochemical Science*, vol. 8, no. 5, pp. 7138–7155, 2013, doi: 10.1016/S1452-3981(23)14836-X.
- [7] M. A. Ameer, E. Khamis, and G. Al-Senani, “Effect of temperature on the stability of adsorbed inhibitors on steel in phosphoric acid solution,” *Journal of Applied Electrochemistry*, vol. 32, no. 2, pp. 149–156, 2002, doi: 10.1023/A:1014777726624.
- [8] Y. Abboud, O. Tanane, A. El Bouari, R. Salghi, B. Hammouti, A. Chetouani, and S. Jodeh, “Corrosion inhibition of carbon steel in hydrochloric acid solution using pomegranate leave extracts,” *Corrosion Engineering, Science and Technology*, early access, pp. 1–9, 2016, doi: 10.1179/1743278215Y.0000000058.
- [9] H. Tyagi and A. Biswas, “A comparative study of copper corrosion inhibition in various industrial environments,” *Journal of Adhesion Science and Technology*, early access, pp. 1–44, 2025, doi: 10.1080/01694243.2025.2491654.
- [10] H. Bairagi, P. Vashishth, G. Ji, S. K. Shukla, E. E. Ebenso, and B. Mangla, “Polymers and their composites for corrosion inhibition application: Development, advancement, and future scope—A critical review,” *Corrosion Communications*, vol. 15, pp. 79–94, 2024, doi: 10.1016/j.corcom.2023.10.006.
- [11] U. V. Agbogo, B. M. Dauda, O. K. Sunmonu, O. C. Elobuiké, and I. M. Inuwa, “Influence of renewable polymer/modifier composition and processing on the properties of multifunctional adhesive leather bonds from PVAc,” *Journal of Multidisciplinary Engineering Science Studies*, vol. 6, 2020. [Online]. Available: <https://www.jmess.org/wp-content/uploads/2020/03/JMESSP13420623.pdf>
- [12] R. M. Hassan, S. M. Ibrahim, H. D. Takagi, and S. A. Sayed, “Kinetics of corrosion inhibition of aluminum in acidic media by water-soluble natural polymeric chondroitin-4-sulfate as anionic polyelectrolyte inhibitor,” *Carbohydrate Polymers*, vol. 192, pp. 356–363, 2018, doi: 10.1016/j.carbpol.2018.03.066.
- [13] K. S. Khairou, A. A. Alfi, and E. M. Mabrouk, “Natural polymers as corrosion inhibitors for aluminium and tin in acidic media,” *Material Science Research India*, vol. 4, no. 2, pp. 279–290, 2007, doi: 10.13005/msri/040207.

- [14] T. Brindha, K. Parimalagandhi, and J. Mallika, "Thermodynamic and electrochemical analysis of synergistic corrosion inhibition performance of natural polysaccharides with metal halides on mild steel in hydrochloric acid solution," *Journal of Bio- and Tribo-Corrosion*, vol. 6, no. 1, Art. no. 3, 2020, doi: 10.1007/s40735-019-0296-7.
- [15] Z. Ghehsareh, T. Sayah, M. Moharramnejad, A. Rahimitabar, and A. Ehsani, "Green guardians: A comprehensive review of environmentally friendly corrosion inhibitors from plant extract to ionic liquids in industrial applications," *Progress in Organic Coatings*, vol. 201, Art. no. 109146, 2025, doi: 10.1016/j.porgcoat.2025.109146.
- [16] Y. El-Etre, "Inhibition of aluminum corrosion using *Opuntia* extract," *Corrosion Science*, vol. 45, no. 11, pp. 2485–2495, 2003, doi: 10.1016/S0010-938X(03)00066-0.
- [17] B. Obot and N. O. Obi-Egbedi, "Adsorption properties and inhibition of mild steel corrosion in sulphuric acid solution by ketoconazole: Experimental and theoretical investigation," *Corrosion Science*, vol. 52, no. 1, pp. 198–204, 2010, doi: 10.1016/j.corsci.2009.09.002.
- [18] M. Abdallah, H. M. Eltass, M. A. Hegazy, and H. Ahmed, "Adsorption and inhibition effect of novel cationic surfactant for pipelines carbon steel in acidic solution," *Protection of Metals and Physical Chemistry of Surfaces*, vol. 52, no. 4, pp. 721–730, 2016, doi: 10.1134/S207020511604002X.
- [19] M. Jiang *et al.*, "New strategies for synergistic inhibition of mild steel corrosion by dual-functionalized chitosan: Film formation and Fe<sup>2+</sup> adsorption," *Journal of Cleaner Production*, vol. 538, Art. no. 147371, 2026, doi: 10.1016/j.jclepro.2025.147371.
- [20] N. U. S. Riyaz, A. Ben Ali, M. Khaled, I. Hussein, and S. Al-Meer, "Chitosan-derived green corrosion inhibitor for carbon steel in CO<sub>2</sub>-saturated media: A graph convolutional network approach," *Industrial & Engineering Chemistry Research*, vol. 65, no. 5, pp. 2479–2492, 2026, doi: 10.1021/acs.iecr.5c03881.
- [21] N. Kumar, P. Anunay, S. Kumar, L. K. Meena, and D. Singh, "An overview on emerging green organic corrosion inhibitors: Sustainable solution for oil and gas industrial applications," *RSC Advances*, vol. 16, no. 5, pp. 3909–3948, 2026, doi: 10.1039/D5RA08166A.
- [22] N. J. Mohammed, M. R. Yusop, and N. K. Othman, "Green and nano-based strategies for controlling mild steel corrosion in acidic media: A systematic review," *npj Materials Degradation*, vol. 10, no. 1, Art. no. 16, 2026, doi: 10.1038/s41529-025-00726-z.
- [23] Y. Liu *et al.*, "Recent progress in organic inhibitors for anticorrosion in complex acid environments," *Coatings*, vol. 16, no. 2, Art. no. 150, 2026, doi: 10.3390/coatings16020150.
- [24] C. Verma, Promila, I. Barsoum, K. Y. Rhee, and A. Alfantazi, "Physicochemical bonding and corrosion protection: Non-covalent and coordination bonds in transport and adsorption of corrosion inhibitors," *Coordination Chemistry Reviews*, vol. 548, Art. no. 217154, 2026, doi: 10.1016/j.ccr.2025.217154.
- [25] S. A. Ghraibit, T. A. Salman, and S. M. Ahmad, "Expired dantrolene drug as sustainable corrosion inhibitor of mild steel in acidic medium," *Journal of Molecular Graphics and Modelling*, vol. 142, Art. no. 109171, 2026, doi: 10.1016/j.jmkgm.2025.109171.
- [26] G. Wang *et al.*, "Elevated-temperature corrosion inhibition of mild steel in sulfuric acid by coupled effects of imidazoline-type inhibitor and thiourea derivatives," *Journal of Materials Science & Technology*, vol. 240, pp. 233–249, 2026, doi: 10.1016/j.jmst.2025.05.004.
- [27] V. U. Agbogo, E. R. Sadiku, L. M. Mavhungu, and M. L. Teffo, "Next-generation biodegradable polymers: Toward a circular plastics economy," *AIMS Bioengineering*, vol. 12, no. 4, pp. 473–502, 2025, doi: 10.3934/bioeng.2025023.

- [28] V. U. Agbogo, E. R. Sadiku, L. Mavhungu, W. K. Kupolati, M. L. Teffo, and O. M. Injor, "Leveraging nanopolymer bio-coatings for biodegradable implant systems: An overview," *Results in Materials*, vol. 29, Art. no. 100868, 2026, doi: 10.1016/j.rinma.2025.100868.
- [29] P. Kumari, S. A. Rao, D. Nayak, and S. E. Peter, "Corrosion mitigation of mild steel in acid media using a potential hydrazide derivative: Experimental and theoretical investigation," *Arab Journal of Basic and Applied Sciences*, vol. 33, no. 1, pp. 32–50, 2026, doi: 10.1080/25765299.2025.2611463.
- [30] C. Verma, A. Singh, and A. Alfantazi, "Benzopyran derivatives as polydentate chelating corrosion inhibitors: Natural products-based  $\sigma$ -donors and  $\pi$ -acceptor ligands," *Coordination Chemistry Reviews*, vol. 548, Art. no. 217191, 2026, doi: 10.1016/j.ccr.2025.217191.
- [31] Kaur, P. Ahluwalia, and H. Singh, "Cassava: Extraction of starch and utilization of flour in bakery products," *International Journal of Food and Fermentation Technology*, vol. 6, no. 2, p. 351, 2016, doi: 10.5958/2277-9396.2016.00059.3.
- [32] S. Z. Kazaure *et al.*, "Kinetics and thermodynamic study of inhibition potentials by ethoxyethane extracts of *Cochlospermum tinctorium* for the oxoacid corrosion of mild steel," *International Journal of Materials and Chemistry*, vol. 5, no. 3, pp. 64–76, 2015. [Online]. Available: <http://article.sapub.org/10.5923.j.ijmc.20150503.03.html>
- [33] N. O. Eddy, A. O. Odiongenyi, E. E. Ebenso, R. Garg, and R. Garg, "Plant wastes as alternative sources of sustainable and green corrosion inhibitors in different environments," *Corrosion Engineering, Science and Technology*, vol. 58, no. 5, pp. 521–533, 2023, doi: 10.1080/1478422X.2023.2204260.
- [34] A. Toghan, H. S. Gadow, A. Fawzy, H. Alhussain, and H. Salah, "Adsorption mechanism, kinetics, thermodynamics, and anticorrosion performance of a new thiophene derivative for C-steel in 1.0 M HCl: Experimental and computational approaches," *Metals*, vol. 13, no. 9, Art. no. 1565, 2023, doi: 10.3390/met13091565.
- [35] A. Tang *et al.*, "Adsorption performance of silica-supported polyamidoamine dendrimers for Cd(II) and Cu(II) in *N,N*-dimethylformamide," *Journal of Molecular Liquids*, vol. 357, Art. no. 119098, 2022, doi: 10.1016/j.molliq.2022.119098.
- [36] S. Sharma and A. Kumar, "Recent advances in metallic corrosion inhibition: A review," *Journal of Molecular Liquids*, vol. 322, Art. no. 114862, 2021, doi: 10.1016/j.molliq.2020.114862.
- [37] P. Vashishth, H. Bairagi, R. Narang, S. K. Shukla, and B. Mangla, "Thermodynamic and electrochemical investigation of inhibition efficiency of green corrosion inhibitor and its comparison with synthetic dyes on MS in acidic medium," *Journal of Molecular Liquids*, vol. 365, Art. no. 120042, 2022, doi: 10.1016/j.molliq.2022.120042.
- [38] M. R. Laamari, J. Benzakour, F. Berrekhis, A. Derja, and D. Villemin, "Adsorption and corrosion inhibition of carbon steel in hydrochloric acid medium by hexamethylenediamine tetra(methylene phosphonic acid)," *Arabian Journal of Chemistry*, vol. 9, pp. S245–S251, 2016, doi: 10.1016/j.arabjc.2011.03.018.
- [39] S. A. Umoren, U. M. Eduok, and E. E. Oguzie, "Corrosion inhibition of mild steel in 1 M H<sub>2</sub>SO<sub>4</sub> by polyvinyl pyrrolidone and synergistic iodide additives," *Portugaliae Electrochimica Acta*, vol. 26, no. 6, pp. 533–546, 2007, doi: 10.4152/pea.200806533.
- [40] M. Christov and A. Popova, "Adsorption characteristics of corrosion inhibitors from corrosion rate measurements," *Corrosion Science*, vol. 46, no. 7, pp. 1613–1620, 2004, doi: 10.1016/j.corsci.2003.10.013.
- [41] O. Sanni, A. P. I. Popoola, and O. S. I. Fayomi, "Temperature effect, activation energies and adsorption studies of waste material as stainless-steel corrosion inhibitor in sulphuric acid 0.5

- M,” *Journal of Bio- and Tribo-Corrosion*, vol. 5, no. 4, Art. no. 88, 2019, doi: 10.1007/s40735-019-0280-2.
- [42] D. Q. Huong, T. Duong, and P. C. Nam, “Effect of the structure and temperature on corrosion inhibition of thiourea derivatives in 1.0 M HCl solution,” *ACS Omega*, vol. 4, no. 11, pp. 14478–14489, 2019, doi: 10.1021/acsomega.9b01599.
- [43] D. Prabhu, P. R. Prabhu, and P. Rao, “Thermodynamics, adsorption, and response surface methodology investigation of the corrosion inhibition of aluminum by *Terminalia chebula* Ritz. extract in H<sub>3</sub>PO<sub>4</sub>,” *Chemical Papers*, vol. 75, no. 2, pp. 653–667, 2021, doi: 10.1007/s11696-020-01318-8.
- [44] F. M. Mahgoub, F. M. Al-Nowaiser, and A. M. Al-Sudairi, “Effect of temperature on the inhibition of the acid corrosion of steel by benzimidazole derivatives,” *Protection of Metals and Physical Chemistry of Surfaces*, vol. 47, no. 3, pp. 381–394, 2011, doi: 10.1134/S2070205111030087.

---

Received: February 11, 2026

Accepted: April 21, 2026